Cancer Biol Med 2019. doi: 10.20892/j.issn.2095-3941.2019.0115

ORIGINAL ARTICLE

Inactivation of FOXO1 induces T follicular cell polarization and involves angioimmunoblastic T cell lymphoma

Meifang Xu[1*], Fei Wang[2*], Hong Chen[3], Lin Liu[4], Wenwen Liu[4], Yinghong Yang[1], Qiaoling Zheng[1], Lihong Zhang[5], Xiaoxuan Li[5], Suxia Lin[5,6], Shengbing Zang[5,6]

[1]Department of Pathology, Fujian Medical University Union Hospital, Fuzhou 350001, China; [2]Division of Pediatrics, University of Texas MD Anderson Cancer Center, Houston, TX 77030, USA; [3]Department of Pathology, The First Affiliated Hospital of Fujian Medical University, Fuzhou 350004, China; [4]Department of Pathology, Fujian Medical University, Fuzhou 350004, China; [5]Sun Yat-sen University Cancer Center, State Key Laboratory of Oncology in South China, Collaborative Innovation Center for Cancer Medicine, Guangzhou 510060, China; [6]Department of Pathology, Sun Yat-sen University Cancer Center, Guangzhou 510060, China

ABSTRACT

Objective: Angioimmunoblastic T cell lymphoma (AITL) is an aggressive form of non-Hodgkin lymphoma derived from mature T cells. However, the underlying pathogenesis of AITL remains unresolved. We aimed to explore the role of FOXO1-mediated signaling in the tumorigenesis and progression of AITL.

Methods: FOXO1 expression was assessed using immunohistochemistry on a total of 46 AITL tissue samples. Retroviruses encoding FOXO1 shRNA were used to knockdown FOXO1 expression in $CD4^+$ T cells. Flow cytometric assays analyzed the proliferation and survival of FOXO1 knockdown $CD4^+$ T cells. Furthermore, we performed adoptive T-cell transfer experiments to identify whether inactivation of FOXO1 induced neoplastic follicular-helper T (Tfh) cell polarization and function.

Results: Patients with low FOXO1 protein levels were prone to have an advanced tumor stage ($P = 0.049$), higher ECOG ps ($P = 0.024$), the presence of bone marrow invasion ($P = 0.000$), and higher IPI ($P = 0.035$). Additionally, the survival rates of patients in the FOXO1 high-expression group were significantly better than those in the FOXO1 low-expression group ($\chi^2 = 5.346$, $P = 0.021$). We also observed that inactivation of FOXO1 increased $CD4^+$ T cell proliferation and altered the survival and cell-cycle progression of $CD4^+$ T cells. Finally, we confirmed that inactivation of FOXO1 induces Tfh cell programing and function.

Conclusions: Inactivation of FOXO1 in AITL plays a key role in the tumorigenesis and progression of AITL. We propose that FOXO1 expression could be a useful prognostic marker in AITL patients to predict poor survival, and to design appropriate therapeutic strategies.

KEYWORDS Angioimmunoblastic T cell lymphoma; FOXO1; inactivation; differentiation

Introduction

Angioimmunoblastic T cell lymphoma (AITL) is an aggressive form of non-Hodgkin lymphoma derived from T follicular-helper (Tfh) cells with unique histology: prominent arborization of endothelial venules, increased follicular-dendritic meshworks, and a polymorphous cellular infiltrate, including EBV-positive B immunoblasts and neoplastic Tfh cells[1-3]. Patients with AITL often show autoimmune manifestations (e.g., hemolytic anemia, rheumatoid arthritis or autoimmune thyroiditis) and have limited responses to intensive chemotherapy, and high relapse rates[4,5]. Identification and validation of targeted therapeutics and a thorough mechanistic understanding of the molecular pathogenesis of AITL is of critical importance.

Forkhead box (FOX) proteins are a large family of Forkhead transcriptional regulators characterized by a conserved 110-aminoacid DNA binding motif termed the "forkhead box" or "winged helix" domain[6]. Among these, mammalian members of class 'O' transcription factors (FOXO), a subgroup of the FOX proteins, including FoxO1, Fox3a, FoxO4 and FoxO6, play roles in the processes of cell proliferation, differentiation, apoptosis, DNA repair, and metabolism[7-9]. Recently Zang et al.[10] showed that coexistence of somatic mutations in the RHO GTPase ($RHOA^{G17V}$) and 5-methylcytosine oxidase TET2 cooperatively modulated

*These authors contributed equally to this work.

Correspondence to: Shengbing Zang
E-mail: zangsb@sysucc.org.cn

Received March 21, 2019; accepted June 24, 2019.
Available at www.cancerbiomed.org

FOXO1 activity and further disrupted peripheral T cell homeostasis and caused immunoinflammatory responses that are commonly associated with AITL. However, the role of FOXO1-mediated signaling in the tumorigenesis and progression of AITL has not been well-defined.

In this study, we investigated the expression of FOXO1 in AITL patients and studied its role in progression and survival of AITL. We also showed the inactivation of FOXO1 polarized $CD4^+$ T cell toward Tfh cells, which are the cell-of-origin of AITL.

Materials and methods

Patient samples

This study retrospectively analyzed 46 newly diagnosed AITL patients at the First Affiliated Hospital of Fujian Medical University and Fujian Medical University Union Hospital from January 2009 to September 2017 and was approved by the Ethics Committee of Fujian Medical University (Approval No. 2017KY087). Written informed consent was obtained from all patients. The handling of human tissue specimens was in strict accordance with the relevant institutional and national guidelines and regulations. AITL tissues were obtained from 46 patients who underwent surgical biopsy and comprised 33 men and 13 women ranging in age from 45 – 84 years (average age 64 years). None of the patients received preoperative chemotherapy or radiation therapy. The diagnosis of AITL was established from the histopathological and immunohistochemical report from two experienced hematopathologists (Hchen and Mxu), according to 2012 WHO criteria. The international prognostic index (IPI) for PTCL scores was applied to assign risk stratification[11]. Forty normal lymph nodes from patients with inflammatory disease at the First Affiliated Hospital of Fujian Medical University were used as controls. Specimens were fixed in 10% neutral formalin and embedded in paraffin.

Animals

All animals were housed at Fujian Medical University. Four-week-old female C57BL/6 and T-cell receptor (TCR) $\alpha^{-/-}$ mice were purchased from Shanghai Animal Center (Shanghai, China). The mice were maintained in temperature-controlled clean racks with a 12-h light/dark cycle. The animals were allowed to acclimatize for 1 week before the start of the experiment. All animal procedures were conducted in full accordance with the Guidelines for the Care and Use of Laboratory Animals, and they were approved by the Institutional Animal Care and Use Committees at Sun Yat-set University Cancer Center.

Follow-up

Complete follow-up information for 46 patients was acquired until September 2018, and the median observation time was 8 months (range: 1–69 months). Overall survival (OS) was defined as the interval between AITL diagnosis and death or the last follow-up.

Immunohistochemistry

Immunohistochemistry (IHC) was performed using the EliVision™ Plus two-step system (Maixin Biotech, Fuzhou, China)according to the manufacturer's instructions. The slides were deparaffinized, rehydrated, and immersed in 3% hydrogen peroxide solution for 10 min. They were then boiled in citrate buffer (pH 6.0) for 3 min and cooled at room temperature for 1 h. Blocking was carried out with 10% normal goat serum at 37°C for 30 min. The slides were then incubated in a 1 : 400 dilution of rabbit monoclonal anti-human/mouse FOXO1 antibody (Cell Signaling Technology, MA, USA) for 1 h at 37°C, followed by three washes with PBS. The slides were incubated with polymerized HRP-anti rabbit lgG and visualized with DAB. Counterstaining was carried out with hematoxylin. Negative control sections were incubated with preimmune serum. PBS was substituted for primary antibody to serve as a blank control.

Mouse T cell isolation

As described previously[10], T cells were isolated by Dynabeads Untouched Mouse T cell kit (ThermoFisher Scientific, MA, USA). Mouse $CD4^+$ T-cells were purified using a $CD4^+$ T cell isolation kit (mouse) (Miltenyi Biotec, Germany). In brief, spleens and lymph nodes were isolated from C57BL/6 mice (6-8 weeks-old) and ground with a syringe plunger to release splenocytes and lymphocytes into a culture dish. The homogenized cell suspensions were filtered with a cell strainer (nylon mesh with 70 μM pores) to remove debris. The suspended cells were centrifuged and the red blood cells were lysed with ACK lysis buffer. The residual cells were then purified by T cell isolation kits following the manufacturer's instructions. The purity of the isolated T cells was assessed by flow cytometric analysis.

Plasmid construction and retrovirus transduction

Based on the mouse *FOXO1* gene sequence in GenBank

(NM_019739) and shRNA design principles, two sequences (shRNA1 and shRNA2) that specifically inhibited *FOXO1* mRNA were designed and cloned into the MSCV-IRES-GFP plasmid vector between the AgeI and EcoRI restriction endonuclease sites. A nonspecific shRNA was used as a negative control (NC). All plasmids were verified by Sanger DNA sequencing. Correctly assembled plasmids were prepared using PureLink HiPure Plasmid Maxiprep kit (Thermo Fischer Scientific, MA, USA).

Retroviruses encoding *FOXO1* shRNA or control shRNA were generated using MSCV and EcoPack plasmids transfected into the potent retroviral packaging cell line, Plat-E (Cell Biolabs, Inc, San Diego, CA), which was maintained in Dulbecco modified Eagle medium (DMEM) supplemented with 10% fetal calf serum (FCS), 1% penicillin/streptomycin, and 1% glutamine. Retrovirus-containing supernatants were collected from transfected Plat-E cells and then concentrated by ultracentrifugation (Beckman SW28 rotor, 20,000 rpm for 2 h at 4°C). Concentrated retroviruses were re-suspended, aliquoted, and stored at -80°C for up to 2 months.

After 12–24 h stimulation of CD4+ cells, concentrated retroviruses at optimized titers, along with polybrene (6 μg/mL, EMD Millipore, MA, USA), were added to cultured T cells, followed by centrifugation (2,000 rpm at 37°C for 90 min). The transduction efficiency of retroviruses was examined by flow cytometry 24–48 h after transduction.

Adoptive T-cell transfer

As described previously[10], isolated total $CD4^+$ T cells in 200 μL PBS were retro-orbitally injected into $TCR\alpha^{-/-}$ mice (6-8 weeks-old, of either sex; 1 million cells /mouse). The reconstitution efficiency of T cells was assessed by examining the GFP fluorescence signals from peripheral blood in recipient mice 4 weeks after adoptive cell transfer.

Flow cytometry analysis

Cells were re-suspended in FACS buffer (PBS with 1% BSA, 2 mM EDTA) and incubated with Fc blocker for 10 min on ice. After washing with FACS buffer, cells were incubated with the desired antibodies at optimal concentrations for 20 min on ice in the dark. Cells were then washed with FACS buffer twice and re-suspended in 200 μL FACS buffer for flow cytometry analysis (LSRII, BD Biosciences, NJ, USA). For intracellular staining, cells were stained with surface markers as described above, treated with cell fixation/permeabilization kit reagents (BD Biosciences, NJ, USA) and then incubated with antibodies for desired intracellular markers. CD4-PE, CD4-APC, or CD4-eFluor 450 was purchased from BD Biosciences. Tfh cell staining was performed using a three-step staining protocol[12]. Annexin V-pacific Blue (Biolegend, CA, USA) was used to assess the apoptotic status of cells. CellTrace Violet (CTV) (Thermo Fisher Scientific, MA, USA) was applied to identify cell proliferation status, and the proliferation index was calculated following the manufacturer's instructions. Cell cycle status was assessed by 7-AAD (Tonbo Biosciences, CA, USA) and BrdU (Biolegend, CA, USA) staining. Flow cytometry analysis was performed using a LSRII platform (BD Biosciences, NJ, USA) and data were analyzed using FlowJo software 7.6 (TreeStar, CA, USA).

Real-time RT-qPCR

RNA was isolated from cell lysates using RNeasy Mini Kit (Qiagen, Germany) as per the manufacturer's instructions, followed by reverse transcription using an AmfiRivert Platinum One cDNA Synthesis Master Mix (GenDEPOT, TX, USA). Diluted cDNA was analyzed by qPCR using z Roche LightCycler 96 real-time PCR system and amfiSure qGreen Q-PCR Master Mix reagents (GenDEPOT, TX, USA). Data were analyzed using the LightCycler software. *FOXO1* mRNA relative expression levels (in fold) were calculated using the $2^{-\Delta\Delta Ct}$ method. Gene expression levels were normalized to *GAPDH*. Primer sequences used for RT-qPCR were as listed below:

FOXO1 forward: 5'-ACATTTCGTCCTCGAACCAGC TCA-3';

FOXO1 reverse: 5'-ATTTCAGACAGACTGGGCAGC GTA3'.

GAPDH forward: 5'-ACCACAGTCCATGCCATCAC-3';

GAPDH reverse: 5'-TCCACCACCCTGTTGCTGTA-3'.

Western blot

Cells were lysed with RIPA buffer (150 mM NaCl, 50 mM Tris-HCl, pH 8.0, 1% Triton X-100, 0.5% sodium deoxycholate and 0.1% SDS) supplemented with protease inhibitor cocktail (GenDEPOT, TX, USA) and incubated on ice for 20 min. Cell debris was removed by centrifuging at 12,000 rpm for 10 min at 4°C. Protein concentrations were measured using a Pierce BCA protein assay kit (Thermo Fisher Scientific, MA, USA). Samples were mixed with SDS sample buffer at 95°C for 10 min. Whole cell lysates were resolved by 10% or 15% SDS-PAGE and transferred to nitrocellulose membranes. Proteins were detected by immunoblotting in TBST (150 mM NaCl, 10 mM Tris-Cl, pH 8.0, 0.5% Tween-20) containing 5% low-fat milk,

followed by incubation with rabbit monoclonal anti-human/mouse FOXO1 antibody (1 : 1,000, Cell Signaling Technology, MA, USA), rabbit monoclonal anti-human/mouse Cyclin D1 antibody (1 : 500, Cell Signaling Technology, MA, USA), rabbit monoclonal anti-mouse p21 antibody (1 : 1,000, Abcam, Cambridge, UK), rabbit polyclonal anti-mouse Caspase3 antibody (1 : 500, Abcam, Cambridge, UK), or rabbit monoclonal anti-mouse β-Actin antibody (1 : 1,000, Sigma, CA, USA) at RT for 1 h. Then, the membrane was incubated with HRP-conjugated secondary antibody (goat anti-mouse IgG HRP, Sigma, CA, USA) and proteins were detected using the West-Q Pico Dura ECL kit (GenDEPOT, TX, USA).

Statistical analysis

Statistically significant differences between and among groups were assessed using χ^2 test or one-way analysis of variance (ANOVA) with the statistical software SPSS version 19.0 (SPSS Inc., Armonk, NY, USA). Survival rates were calculated by the Kaplan-Meier method, and comparisons of survival curves were performed by the log-rank test. *P* values less than 0.05 were considered to be statistically significant.

Results

Clinical characteristics

Clinical characteristics of the patients are summarized in **Table 1**. Thirty-three patients were male, accounting for 71.7%. A total of 28 (60.9%) patients were scored ≥ 2 by the ECOG performance status (ps). The median age at diagnosis was 67 (range 45–84) and 80.4% (37/46) patients were older than 60 years. Among the patients, 90.0% (40/46) of the diagnoses were estimated as being at an advanced stage. Mediastinal (80.4%), Cervical (67.4%), or inguinal (21.7%) lymph nodes were involved. Thirty-six patients (78.3%) had been found with two different sites of lymph node enlargement. Anemia (hemoglobin < 120 g/L) and leukocytosis (white blood cell count > 10×10^9 L^{-1}) were observed in 58.7% (n = 27) and 21.7% (n = 10) patients, respectively. Serum lactate dehydrogenase (LDH) was found elevated in 58.7% (n = 27) of the patients. Patients with bone marrow involvement represented 45.7%. Seventeen patients (40.0%) had skin rash and 24 patients (52.2%) had subcutaneous edema. Twenty patients (43.5%) had ascites. Nine patients (19.6%) had arthritis. Hepatomegaly (21.7%) and splenomegaly (47.8%) were common in AITL patients. Other extranodal sites were uncommon, including lung (n = 2), and intestine (n =1).

Patients were stratified into 3 risk subgroups by IPI score[11]: 2.2% (n = 1) were at low risk, 30.4% (n = 14) were at intermediate risk, and 67.4% (n = 31) were at high risk, depending on the numbers of adverse prognostic factors (1, 2, 3–4).

Low FOXO1 expression correlates with aggressive clinicopathological features and poor prognosis of AITL

In normal lymph nodes, IHC immuostaining of FOXO1 was almost exclusively detected in the nucleus (**Figure 1A**). Among the 46 AITL cases assessed by IHC staining, 11 tumor samples displayed heterogeneous nuclear staining (**Figure 1B**),

Table 1 Clinic and biologic characteristics of the patients

Characteristics	No. of patients (n = 46)
Gender (male/female)	33/13
Age, median (range, years)	67 (45–84)
OS (months)	8 (1–69)
LN involvement (%)	
Cervical	31 (7.4%)
Mediastinal	37 (80.4%)
Inguinal	10 (21.7%)
Two different sites	36 (78.3%)
Extranodal involvement (%)	
Anemia	27 (58.7%)
Leukocytosis	10 (21.7%)
LDH (higher than normal)	27 (58.7%)
Bone marrow	21 (45.7%)
Skin rash	17 (40.0%)
Edema	24 (52.2%)
Arthritis	9 (19.6%)
Ascites	20 (43.5%)
Splenomegaly	22 (47.8%)
Hepatomegaly	10 (15.2%)
PIT score	
1	1 (2.2%)
2	14 (30.4%)
3	8 (17.4%)
4	23 (50.0%)

14 tumor samples showed variegated staining in both the cytosol and nucleus (**Figure 1C**), 13 cases exhibited dominant staining in the cytosol (**Figure 1D**), and 8 cases were negative (**Figure 1E**). Previous studies have shown that phosphorylated FOXO1 is transported from the nucleus to cytoplasm and then becomes a target for proteasomal degradation to be fully inactivated[13-15]. These results led us to consider cytosolic FOXO1 expression as being in an inactive form. We categorized AITL samples with FOXO1 expression exclusively in cytosol, or FOXO1 negative expression into the FOXO1 low expression group. AITL samples with FOXO1 expression exclusively in nucleus or in both the cytosol and nucleus were grouped into the FOXO1 high expression group. **Table 2** shows the relationship between FOXO1 expression and selected clinicopathologic parameters. FOXO1 expression did not vary significantly with age, gender, LDH level, or systemic symptoms. However, patients with low FOXO1 protein levels were prone to have an advanced stage ($P = 0.049$), higher ECOG ps ($P = 0.024$), the presence of bone marrow invasion ($P = 0.000$), and higher PIT ($P = 0.035$). Thus, low expression of FOXO1 was associated with multiple malignant characteristics of AITL.

From the results of Kaplan-Meier statistical analysis, the survival rates of the FOXO1 high-expression group and the low-expression group both declined progressively. However, the survival rates of the patients in the high-expression group were significantly better than those in the low-expression group, and the differences were statistically significant ($\chi^2 = 5.346$, $P = 0.021$) (**Figure 1F**). Taken together, these data suggested that FOXO1 is associated with malignant characteristics of AITL. Furthermore, low FOXO1 expression may predict poor prognosis in AITL patients.

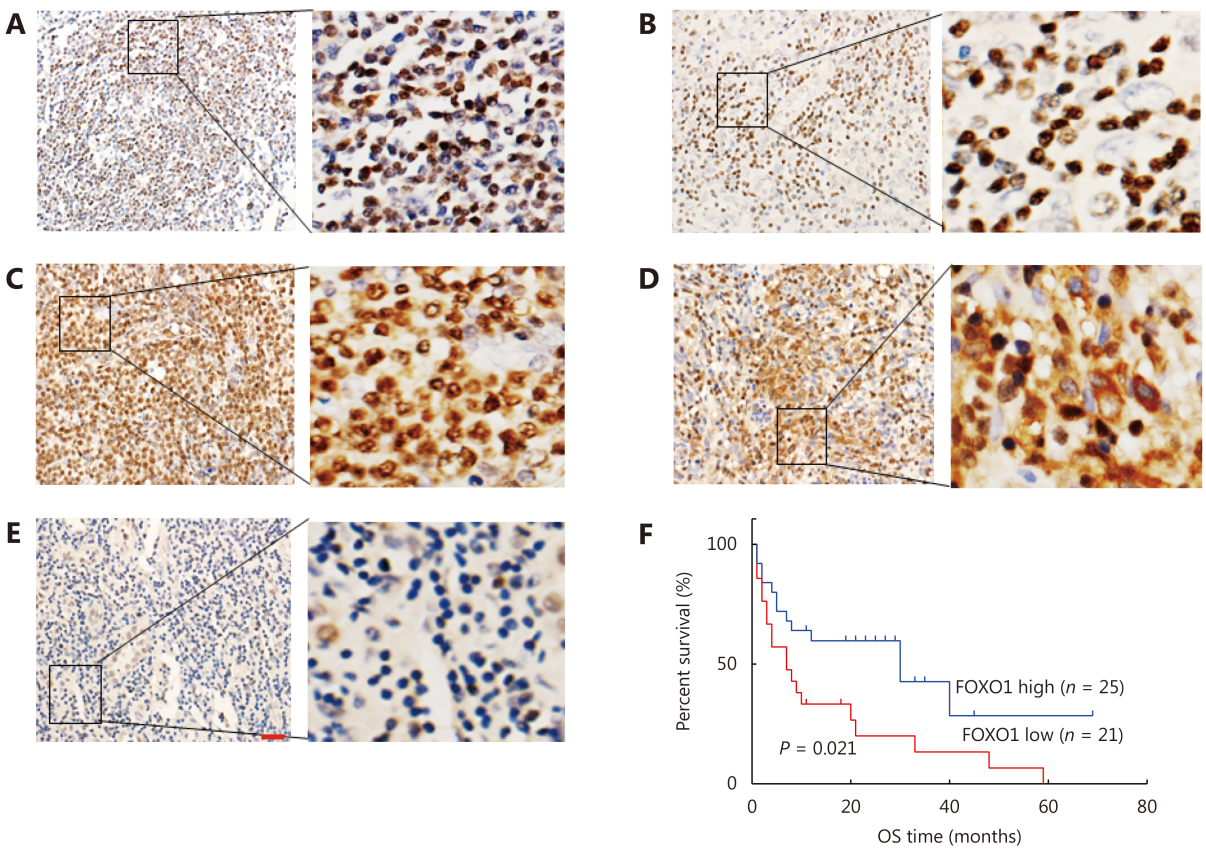

Figure 1 FOXO1 expression exclusively in cytosol or negative in AITL samples correlates with poor prognosis. (A) FOXO1 was almost exclusively detected in the nuclei of lymphocytes in lymph nodes. (B) FOXO1 exhibited heterogeneous nuclear staining in some AITL patients. (C) FOXO1 displayed variegated staining in both the cytosol and nucleus in some AITL patients. (D) FOXO1 exerted dominant staining in the cytosol in some AITL patients. (E) FOXO1 was negative in some AITL patients. (F) Kaplan–Meier analysis of overall survival for AITL patients with high or low FOXO1 expression. EliVision Plus two-step immunohistochemical technique with 3-3′ diaminobenzidine (DAB) staining was used in (A-E)(400 ×; scale bar: 10 μm).

Table 2 Relationship between FOXO1 expression and clinicopathologic characteristics of AITL patients

Characteristics	Cases	FOXO1 expression		χ^2	*P*
		Lower, *n*	Higher, *n*		
Gender					
Male	33	15	18	2.562	0.109
Female	13	10	3		
Age, years					
≤ 60	9	4	5	0.080	0.770
> 60	37	21	16		
ECOG ps					
0–1	18	14	4	5.083	0.024
2–4	28	11	17		
Ann Arbor stage					
I–II	6	6	0	3.873	0.049
III–IV	40	19	21		
LDH level					
Normal	19	14	5	3.641	0.056
High	27	11	16		
Systemic symptoms					
Yes	36	20	16	0.097	0.755
No	10	5	5		
BM involvement					
Involved	21	5	16	12.347	0.000
Not involved	25	20	5		
PIT					
1–2	15	12	3	4.469	0.035
3–4	31	13	18		

Inactivation of FOXO1 in CD4$^+$ T cells increases cell proliferation

Given the close association of FOXO1 with AITL, we hypothesized that inactivation of FOXO1 may play an important role as an oncogenic driver in the pathogenesis of AITL. Firstly, we isolated CD4$^+$ T-cells from C57BL/6 mice and then transduced them with retrovirus encoding either non-specific shRNA-IRES-GFP or FOXO1 shRNA-IRES-GFP. Retrovirus FOXO1 shRNA expression vectors and the non-specific shRNA control vector are listed in **Table 3**. Knockdown of FOXO1 expression in CD4$^+$ T-cells was detected by RT-qPCR and western blot analysis. FOXO1-shRNA1-IRES-GFP and FOXO1-shRNA2-IRES-GFP significantly inhibited *FOXO1* mRNA expression in CD4$^+$ T cells as compared with control shRNA and untransfected CD4$^+$ T cells ($P < 0.01$; **Figure 2A**). The inhibition of FOXO1 protein expression by FOXO1-shRNA1-IRES-GFP or FOXO1-shRNA2-IRES-GFP was confirmed using Western blot analysis (**Figure 2B**). No difference was found between control shRNA and untransfected CD4$^+$ T-cells in mRNA or protein expression.

We then tested the proliferative response of FOXO1 knockdown CD4$^+$ T cells to stimulation with anti-CD3 and

Table 3 The sequences for the single-stranded DNA oligonucleotides of FOXO1 shRNA and non-specific shRNA

shRNA Name	5′	STEMP	Loop	STEMP	3′
FOXO1-shRNA1-F	ccgg	aaGGAACTGGAAAGAGTTCTTGG	TTCAAGAGA	CCAAGAACTCTTTCCAGTTCCtt	TTTTTg
FOXO1-shRNA1-R	aattcaaaaa	aaGGAACTGGAAAGAGTTCTTGG	TCTCTTGAA	CCAAGAACTCTTTCCAGTTCCtt	
FOXO1-shRNA2-F	ccgg	gaGCAACGATGACTTTGATAACT	TTCAAGAGA	AGTTATCAAAGTCATCGTTGCtc	TTTTTg
FOXO1-shRNA2-R	aattcaaaaa	gaGCAACGATGACTTTGATAACT	TCTCTTGAA	AGTTATCAAAGTCATCGTTGCtc	
shRNA-NC-F	ccgg	TTCTCCGAACGTGTCACGT	TTCAAGAGA	AAGAGGCTTGCACAGTGCA	TTTTTg
shRNA-NC-R	aattcaaaaa	TTCTCCGAACGTGTCACGT	TCTCTTGAA	AAGAGGCTTGCACAGTGCA	

anti-CD28 antibodies. After transducing the CD4+ T cells from C57BL/6 mice for 24 h in media with anti-CD3 and anti-CD28 antibodies, we labeled the cells with CellTrace Violet (CTV) and cultured them for a further 3 days. The results revealed a marked increase in cell division of FOXO1 knock-down CD4+ T cells as evaluated by CTV staining, compared to the control CD4+ T cells, indicating that inactivation of FOXO1 promotes TCR-driven proliferation *in vitro* (**Figure 2C**).

Inactivation of FOXO1 alters the survival and

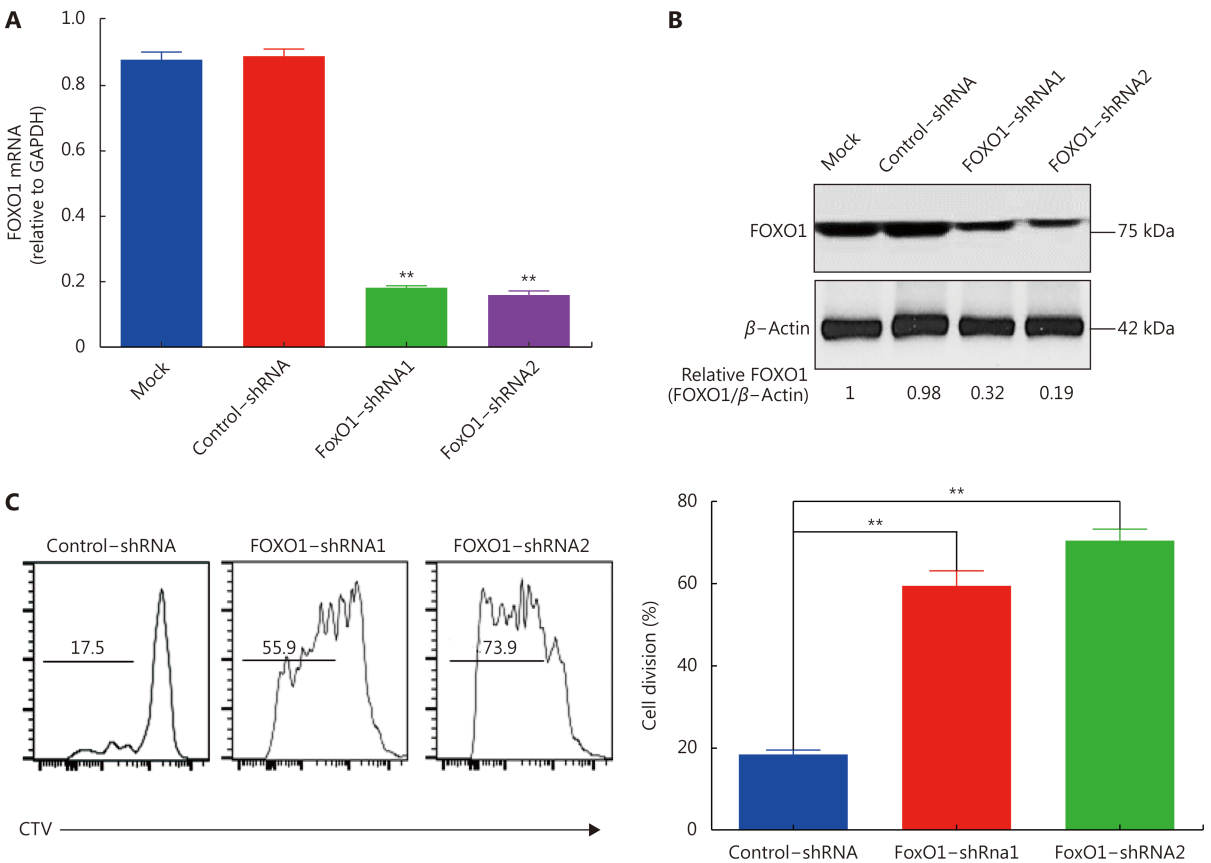

Figure 2 Inactivation of FOXO1 in CD4+ T cells increases cell proliferation. (A and B) Retroviral FOXO1 shRNA expression vectors and non-specific shRNA control vectors were transduced into CD4+ T cells. Knockdown of FOXO1 expression in CD4+ T cells was detected by RT-qPCR (A) and Western blot analysis (B). (C) *In vitro* CellTrace Violet (CTV) proliferation assay of CD4+ T cells transduced with retroviral FOXO1 shRNA or non-specific shRNA control vectors on day 3. The *P* value in (A) was calculated by ANOVA followed by Dunnett's test using triplicate samples from two independent experiments. The *P* value in (C) was calculated by ANOVA followed by Dunnett's test using triplicate samples from two independent experiments. Columns indicate means; bars are the standard error. $^{**}P \leq 0.01$.

cell-cycle progression of CD4+ T cells

To further assess how inactivation of FOXO1 affected the fate of CD4+ T cells, we monitored cell apoptosis in FOXO1 knockdown CD4+ T cells. Compared to control CD4+ T cells, FOXO1 knockdown CD4+ T-cells showed obvious reductions in cell apoptosis (annexin V staining) (**Figure 3A**). In parallel, Fas, a key ligand involved in regulating CD4+ T cell apoptosis upon T-cell receptor activation, was downregulated in FOXO1 knockdown CD4+ T cells (**Figure 3B**). We confirmed the changes in protein levels of cleaved caspase3 in FOXO1 knockdown CD4+ T cells (**Figure 3C**), which was regulated by Fas and mediated cell apoptosis. Cell cycle analysis using 7-AAD plus BrdU staining showed an increase in numbers of FOXO1 knockdown CD4+ T cells in S phase (**Figure 3D**), which agrees with the accelerated proliferation phenotype described above (**Figure 2C**). We also observed a

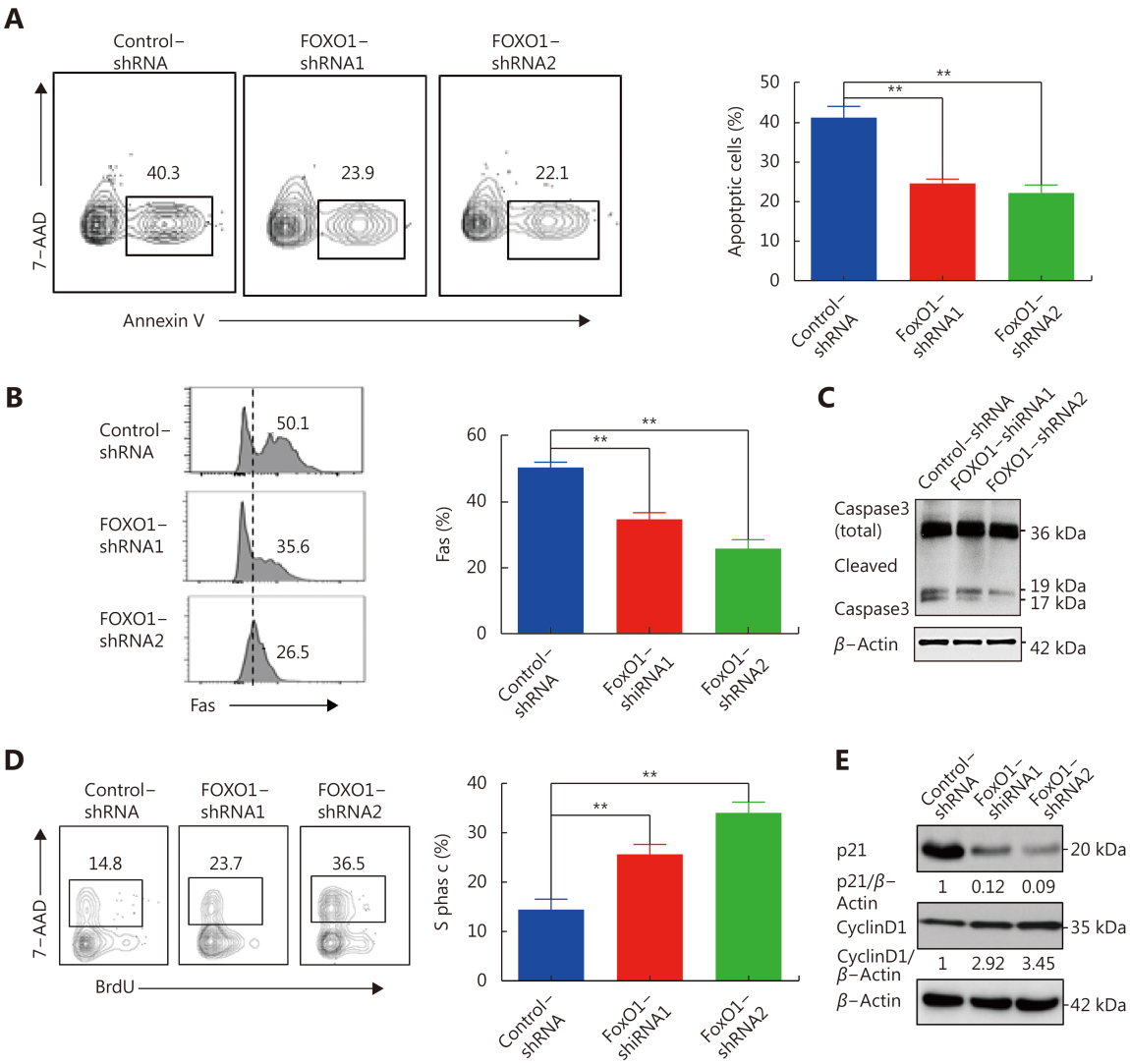

Figure 3 Inactivation of FOXO1 alters the survival and cell-cycle progression of CD4+ T cells. (A and B) Retroviral FOXO1 shRNA expression vectors and non-specific shRNA control vectors were transduced into CD4+ T cells. Annexin V (A) and Fas (B) staining of transferring CD4+ T cells on day 3 were analyzed by flow cytometric analysis. (C) Immunoblots showing the detection of total caspase3 and cleaved caspase3 in transferred CD4+ T cells on day 3. β-actin was used as a loading control. (D) Cell cycle analysis with immunostaining of 7-AAD and BrdU in transferred CD4+ T cells on day 3. The plots represent cell cycle S phase. (E) Immunoblots showing the detection of p21 and cyclinD1 in transferred CD4+ T cells on day 3. The *P* values in (A, B, D) were calculated by ANOVA followed by Dunnett's test using triplicate samples from three independent experiments. Columns indicate means; bars are the standard error. $^{**}P \leq 0.01$.

significant reduction of p21 and upregulation of cyclinD1 in FOXO1 knockdown CD4$^+$ T cells by Western blot (**Figure 3E**). These results strongly support a role of the inactivation of FOXO1 in the inhibition of apoptosis and acceleration of cell cycle in CD4$^+$ T cells.

Inactivation of FOXO1 induces Tfh cell polarization and function

To further investigate the role of FOXO1 in T cell development and the pathogenesis of AITL, we firstly directed naive CD4$^+$ T cell differentiation toward Tfh cells *in vitro*, but differentiation was not successful. Then, we performed adoptive T cell transfer experiments using FOXO1 knockdown CD4$^+$ T cells and control CD4$^+$ T cells. We isolated total CD4$^+$ T cells from lymph nodes and spleens of C57BL/6 mice and then transduced them with retrovirus encoding either non-specific shRNA-IRES-GFP or FOXO1 shRNA-IRES-GFP *in vitro* to yield control CD4$^+$ T cells and FOXO1 knockdown CD4$^+$ T cells. We then retro-orbitally injected them into TCR$\alpha^{-/-}$ mice lacking the majority of endogenous TCRα^+ T cells (**Figure 4A**).

After a follow-up period of 3 months, we found that the spleens and lymph nodes of mice that were injected with FOXO1 knockdown CD4$^+$ T cells were much larger than in the control group (**Figure 4B**). Flow cytometric analysis revealed a most notable increase in the population of Tfh cells (CD4$^+$CXCR5$^+$Bcl6$^+$) in FOXO1 knockdown CD4$^+$ T cells (**Figure 4C**). Furthermore, we observed an increase in the population of germinal center B cells (B220$^+$GL7$^+$Fas$^+$) (**Figure 4D**), which were stimulated by Tfh cells. We also observed elevated serum levels of proinflammatory IL-6 and IL-21 cytokines by ELISA analysis (**Figure 4E**), which were produced by Tfh cells. However, after a 1-year period of follow up, the amount of transferring FOXO1 knockdown CD4$^+$ T cells cells in recipient mice gradually decreased (data not shown), indicating inactivation of FOXO1 alone is insufficient to cause malignant transformation of CD4$^+$ T cells. Nonetheless, these data imply that inactivation of FOXO1 might play an important role in the initial step of development of Tfh-associated malignancies, such as AITL.

Discussion

Recently the combination of whole exome sequencing, RNAseq and deep targeted sequencing has unveiled a new highly prevalent RHOA mutation (RHOA^{G17V}) in almost 70% of AITL cases, most commonly in association with loss of function mutations in the *TET2* tumor suppressor gene[16,17]. Zang et al.[10] have shown that genetic depletion of *TET2*, together with RHOA^{G17V} expression, results in mature CD4$^+$ T cell abnormalities characterized by increased cell proliferation, decreased apoptosis or cell death, aberrant activation of TCR signaling, and an imbalance among Th17, Tregs, and Tfh cells to resemble the inflammatory background in patients with AITL both *in vitro* and *in vivo* by perturbing FOXO1 activity. However, whether loss of FOXO1 expression in AITL patients is associated with tumorigenesis and progression is unknown.

In this study, IHC immuostaining of FOXO1 was almost exclusively detected in the nuclei of normal T-cells in lymph nodes. Interestingly we found FOXO1 localization of IHC staining in AITL samples involved four patterns: nucleus, cytosol, both in cytosol and nucleus, or negative staining. Previous studies have shown that phosphorylated FOXO1 is transported from nucleus to cytoplasm and then becomes a target for proteasomal degradation to be fully inactivated[13-15]. These results led us to consider cytosolic FOXO1 expression as being in an inactive form. We categorized AITL samples with FOXO1 expression exclusively in cytosol, or FOXO1 negative expression into the FOXO1 low expression cohort. AITL patients dramatically lost FOXO1 expression in the nucleus. Patients with low expression of FOXO1 tended to have an advanced stage, high ECOG ps, the presence of bone marrow invasion, and high PIT score. Furthermore, the survival rates of patients with high FOXO1 expression were significantly better than those with low FOXO1 expression. Taken together, low expression of FOXO1 was associated with multiple malignant characteristics of AITL, and appeared to enhance the pathology of AITL, and, consequently, may be of clinical and pharmacological importance as a biomarker for AITL.

Currently the role of FOXO1 in cancer is variable and debatable. FOXO1 is commonly dysregulated in several tumor types including gastric cancer[18,19], breast cancer[20,21], hepatocellular carcinoma (HCC)[22,23], prostate cancer[24,25], and colorectal cancer[26,27]. Nuclear exclusion of FOXO1 was in association with higher microvessel areas and levels of several angiogenesis-related proteins, including hypoxia inducible factor-1α, vessel endothelial growth factor, phosphorylated protein kinase B, and nuclear factor-κB in gastric cancer tissues[19]. In the breast cancer cell line MCF-7, cell proliferation was suppressed after up-regulation of FOXO1 expression to suppress miRNA-223 inducing tumorigenicity[21]. Similarly down regulation of FOXO1 by miR-1269 promotes cell proliferation in HCC[22]. FOXO1-derived peptide FO1-6nls can restore the tumor suppressor function of FOXO1 by specifically opposing CDK1/2-

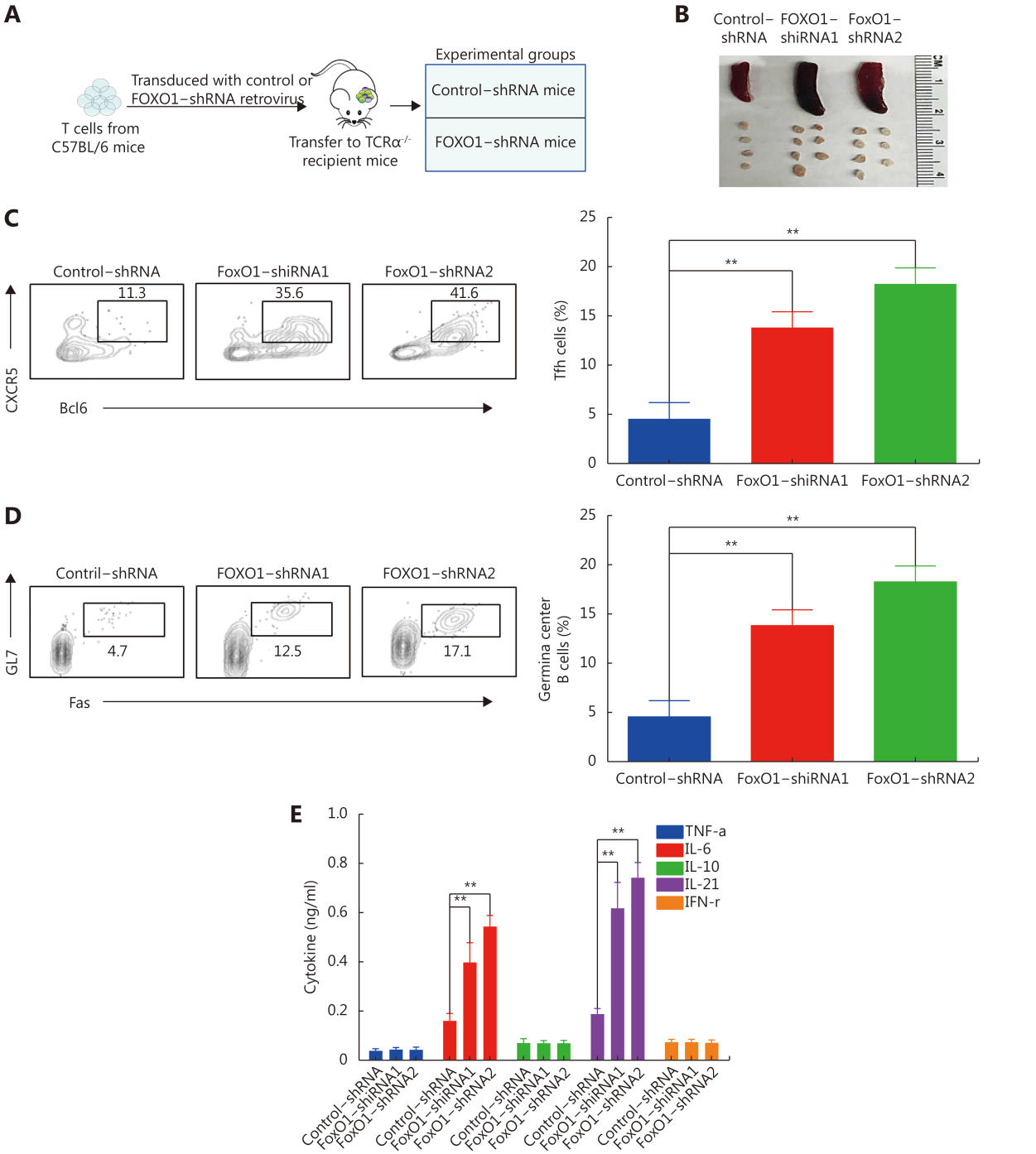

Figure 4 Inactivation of FOXO1 induces Tfh cell polarization and function. (A) Schematic representation of experimental design for adoptive T cell transfer experiments. (B) Representative photographs of spleens and lymph nodes from recipient TCRα$^{-/-}$ mice at 3 months after adoptive transfer of FOXO1 knockdown CD4^{+} T cells or control CD4^{+} T cells. (C and D) Tfh cells (C) and germinal center B cells (D) from TCRα$^{-/-}$ mice at 3 months after adoptive transfer of FOXO1 knockdown CD4^{+} T cells or control CD4^{+} T cells were analyzed by flow cytometry. (E) ELISA showing the detection of serum levels of cytokines from recipient TCRα$^{-/-}$ mice at 3 months after adoptive transfer of FOXO1 knockdown CD4^{+} T cells or control CD4^{+} T cells. The *P* values in (C and D) were calculated by ANOVA followed by Dunnett's test using triplicate samples of 3 mice of each group in two independent experiments. The *P* value in (E) was calculated by ANOVA followed by Dunnett's test for 6 mice of each group. Columns indicate means; bars are the standard error. $^{**}P \leq 0.01$.

mediated phosphorylation and hence may have therapeutic potential in the treatment of prostate cancer[25]. Phosphorylation of FOXO1 is induced by the mTOR inhibitor Rapamycin, which promotes tumor growth in colorectal cancer cells[26]. Collectively, these observations suggest that FOXO1 is a mediator of tumor suppression and a potential biomarker of poor survival of cancer patients. FOXO1 is regulated by the PTEN tumor suppressor and is cytosolic in PTEN-negative renal and prostate carcinoma cells[28]. Overproduction of FOXO1 proteins in PTEN-negative tumor cells has the same effect in promoting cell survival and cellular proliferation as the overexpression of PTEN in these cells[29]. In addition, PTEN-null cells induce tumorigenesis in nude mice, which can be overridden by the expression of a constitutively active form of FOXO1[30]. However, Trinh et al.[31] showed Recurrent FOXO1 mutation in the N-terminal region resulting in nuclear retention was associated with decreased overall survival in diffuse large B-cell lymphoma (DLBCL) patients treated with rituximab, cyclophosphamide, doxorubicin, vincristine, and prednisone, independent of cell of origin and the revised International Prognostic Index. Recurrent FOXO1 mutations, which prevent AKT targeting and lock the transcription factor in the nucleus, circumvent mutual exclusivity between PI3K and FOXO1 activation in Burkitt lymphoma (BL) and demonstrate proproliferative and antiapoptotic activity in BL[32]. These results identify FOXO1 nuclear localization as an oncogenic event and will be a novel prognostic factor that plays an important role in in GC B-cell-derived lymphomagenesis.

In T-cells, antigen recognition activates the PI3K/Akt pathway, resulting in production of the second messenger phosphatidylinositol-3,4,5 trisphosphate, activation of the serine/threonine kinases Akt and SGK1, and the phosphorylation of different substrates actively participating in the translation of these external stimuli into an effective T-cell response[33,34]. Among these substrates, FOXO1 phosphorylation by Akt in the nucleus triggers its relocalization to the cytosol[35,36], thereby shutting down its transcriptional activity. FOXO1 positively controls *Foxp3* gene expression and maintains the proper functioning of Tregs to suppress autoimmunity[37,38]. It has been shown that FOXO1 is a negative regulator of Th17 cells by inhibiting RORγt activity[39] and that inactivation of FOXO1 is essential for Tfh cell differentiation[40]. FOXO1 functions as a transcriptional activator of *PD-1,* which promotes the differentiation of terminally exhausted cytotoxic T lymphocytes (CTLs)[41]. Stone et al.[40] showed ICOS signaling transiently inactivates FOXO1 to initiate a Tfh cell contingency by its regulation of Bcl6. Transcriptional and genomic profiling studies have established a close relationship between AITL and Tfh cells[42,43]. In our study, we observed that inactivation of FOXO1 increased cell proliferation and altered the survival and cell-cycle progression of $CD4^+$ T cells. Furthermore, inactivation of FOXO1 induced Tfh cell programing and functions. Our data indicate that inactivation of FOXO1 plays a particularly important role in the development of Tfh-associated malignancies, such as AITL.

Conclusions

In summary, we show that low expression of FOXO1 in AITL plays key roles in tumor progression, as well as in the incidence of poor survival. We also showed inactivation of FOXO1 increased cell proliferation and altered the survival and cell-cycle progression of $CD4^+$ T cells, and eventually induces Tfh cell programing and functions. Put together, the inactivation of FOXO1 expression could be a useful prognostic marker in AITL patients to predict poor survival and design appropriate therapeutic strategies.

Acknowledgements

This work was supported by Natural Science Foundation of Fujian Province (Grant No. 2015J01314). The authenticity of this article has been validated by uploading the key raw data onto the Research Data Deposit public platform (www.researchdata.org.cn), with the approval RDD number as RDDB2019000584.

Conflict of interest statement

No potential conflicts of interest are disclosed.

References

1. De Leval L, Gisselbrecht C, Gaulard P. Advances in the understanding and management of angioimmunoblastic T-cell lymphoma. Br J Haematol. 2010; 148: 673-89.
2. Cortés JR, Palomero T. The curious origins of angioimmunoblastic T-cell lymphoma. Curr Opin Hematol. 2016; 23: 434-43.
3. Lunning MA, Vose JM. Angioimmunoblastic T-cell lymphoma: the many-faced lymphoma. Blood. 2017; 129: 1095-102.
4. Lemonnier F, Gaulard P, de Leval L. New insights in the pathogenesis of T-cell lymphomas. Curr Opin Oncol. 2018; 30: 277-84.
5. Jaffe ES, Nicolae A, Pittaluga S. Peripheral T-cell and NK-cell lymphomas in the WHO classification: pearls and pitfalls. Mod

Pathol. 2013; 26(Suppl 1): S71-87.
6. Clark KL, Halay ED, Lai E, Burley SK. Co-crystal structure of the HNF-3/*fork head* DNA-recognition motif resembles histone H5. Nature. 1993; 364: 412-20.
7. Kaestner KH, Knochel W, Martinez DE. Unified nomenclature for the winged helix/forkhead transcription factors. Genes Dev. 2000; 14: 142-6.
8. Fu Z, Tindall DJ. FOXOs, cancer and regulation of apoptosis. Oncogene. 2008; 27: 2312-9.
9. Coomans de Brachène A, Demoulin JB. FOXO transcription factors in cancer development and therapy. Cell Mol Life Sci. 2016; 73: 1159-72.
10. Zang SB, Li J, Yang HY, Zeng HX, Han W, Zhang JX, et al. Mutations in 5-methylcytosine oxidase TET2 and RhoA cooperatively disrupt T cell homeostasis. J Clin Invest. 2017; 127: 2998-3012.
11. Gallamini A, Stelitano C, Calvi R. Peripheral T-cell lymphoma unspecified (PTCL-U): a new prognostic model from a retrospective multicentric clinical study. Blood. 2004; 103: 2474-9.
12. Chen RQ, Bélanger S, Frederick MA, Li B, Johnston RJ, Xiao NM, et al. In vivo RNA interference screens identify regulators of antiviral $CD4^+$ and $CD8^+$ T cell differentiation. Immunity. 2014; 41: 325-38.
13. Vogt PK, Jiang H, Aoki M. Triple layer control: phosphorylation, acetylation and ubiquitination of FOXO proteins. Cell Cycle. 2005; 4: 908-13.
14. Huang HJ, Regan KM, Lou ZK, Chen JJ, Tindall DJ. CDK2-dependent phosphorylation of FOXO1 as an apoptotic response to DNA damage. Science. 2006; 314: 294-7.
15. Huang HJ, Regan KM, Wang F, Wang DP, Smith DI, van Deursen JMA, et al. Skp2 inhibits FOXO1 in tumor suppression through ubiquitin-mediated degradation. Proc Natl Acad Sci USA. 2005; 102: 1649-54.
16. Yoo HY, Sung MK, Lee SH, Kim S, Lee H, Park S, et al. A recurrent inactivating mutation in RHOA GTPase in angioimmunoblastic T cell lymphoma. Nat Genet. 2014; 46: 371-5.
17. Odejide O, Weigert O, Lane AA, Toscano D, Lunning MA, Kopp N, et al. A targeted mutational landscape of angioimmunoblastic T-cell lymphoma. Blood. 2014; 123: 1293-6.
18. Kim SY, Yoon J, Ko YS, Chang MS, Park JW, Lee HE, et al. Constitutive phosphorylation of the FOXO1 transcription factor in gastric cancer cells correlates with microvessel area and the expressions of angiogenesis-related molecules. BMC Cancer. 2011; 11: 264.
19. Li F, Liu BH, Gao Y, Liu YL, Xu Y, Tong WD, et al. Upregulation of microRNA-107 induces proliferation in human gastric cancer cells by targeting the transcription factor FOXO1. FEBS Lett. 2014; 588: 538-44.
20. Procaccia S, Ordan M, Cohen I, Bendetz-Nezer S, Seger R. Direct binding of MEK1 and MEK2 to AKT induces FOXO1 phosphorylation, cellular migration and metastasis. Sci Rep. 2017; 7: 43078.
21. Wei YT, Guo DW, Hou XZ, Jiang DQ. miRNA-223 suppresses FOXO1 and functions as a potential tumor marker in breast cancer. Cell Mol Biol. 2017; 63: 113-8.
22. Yang XW, Shen GZ, Cao LQ, Jiang XF, Peng HP, Shen G, et al. MicroRNA-1269 promotes proliferation in human hepatocellular carcinoma via downregulation of FOXO1. BMC Cancer. 2014; 14: 909.
23. Jiang JY, Liu Z, Ge C, Chen C, Zhao FY, et al. NK3 homeobox 1 (NKX3.1) up-regulates forkhead box O1 expression in hepatocellular carcinoma and thereby suppresses tumor proliferation and invasion. J Biol Chem. 2017; 292: 19146-59.
24. Wallis CJD, Gordanpour A, Bendavid JS, Sugar L, Nam RK, Seth A. MiR-182 Is Associated with Growth, Migration and Invasion in Prostate Cancer via Suppression of FOXO1. J Cancer. 2015; 6: 1295-305.
25. Lu HR, Liu P, Pan YQ, Huang HJ. Inhibition of cyclin-dependent kinase phosphorylation of FOXO1 and prostate cancer cell growth by a peptide derived from FOXO1. Neoplasia. 2011; 13: 854-63.
26. Abdelnour-Berchtold E, Cerantola Y, Roulin D, Dormond-Meuwly A, Demartines N, Dormond O. Rapamycin-mediated FOXO1 inactivation reduces the anticancer efficacy of rapamycin. Anticancer Res. 2010; 30: 799-804.
27. Wu LH, Li HH, Jia CY, Cheng W, Yu M, Peng M, et al. MicroRNA-223 regulates FOXO1 expression and cell proliferation. FEBS Lett. 2012; 586: 1038-43.
28. Nakamura N, Ramaswamy S, Vazquez F, Signoretti S, Loda M, Sellers WR. Forkhead transcription factors are critical effectors of cell death and cell cycle arrest downstream of PTEN. Mol Cell Biol. 2000; 20: 8969-82.
29. Modur V, Nagarajan R, Evers BM, Milbrandt J. FOXO proteins regulate tumor necrosis factor-related apoptosis inducing ligand expression. J Biol Chem. 2002; 277: 47928-37.
30. Ramaswamy S, Nakamura N, Sansal I, Bergeron L, Sellers WR. A novel mechanism of gene regulation and tumor suppression by the transcription factor FKHR. Cancer Cell. 2002; 2: 81-91.
31. Trinh DL, Scott DW, Morin RD, Mendez-Lago M, An JH, Jones SJ, et al. Analysis of *FOXO1* mutations in diffuse large B-cell lymphoma. Blood. 2013; 121: 3666-74.
32. Kabrani E, Chu VT, Tasouri E, Sommermann T, Baßler K, Ulas T, et al. Nuclear FOXO1 promotes lymphomagenesis in germinal center B cells. Blood. 2018; 132: 2670-83.
33. Costello PS, Gallagher M, Cantrell DA. Sustained and dynamic inositol lipid metabolism inside and outside the immunological synapse. Nat Immunol. 2002; 3: 1082-9.
34. Harriague J, Bismuth G. Imaging antigen-induced PI3K activation in T cells. Nat Immunol. 2002; 3: 1090-6.
35. Fabre S, Lang V, Harriague J, Jobart A, Unterman TG, Trautmann A, et al. Stable activation of phosphatidylinositol 3-kinase in the T cell immunological synapse stimulates Akt signaling to FoxO1 nuclear exclusion and cell growth control. J. Immunol. 2005; 174: 4161-71.
36. Charvet C, Canonigo AJ, Bécart S, Maurer U, Miletic AV, Swat W, et al. Vav1 promotes T cell cycle progression by linking TCR/CD28 costimulation to FOXO1 and p27kip1 expression. J Immunol.

2006; 177: 5024-31.

37. Ouyang WM, Li MO. Foxo: in command of T lymphocyte homeostasis and tolerance. Trends Immunol. 2011; 32: 26-33.
38. Du XR, Shi H, Li J, Dong YL, Liang JL, Ye J, et al. *Mst1*/*Mst2* regulate development and function of regulatory T cells through modulation of Foxo1/Foxo3 stability in autoimmune disease. J Immunol. 2014; 192: 1525-35.
39. Lainé A, Martin B, Luka M, Mir L, Auffray C, Lucas B, et al. Foxo1 Is a T Cell-Intrinsic Inhibitor of the RORγt-Th17 Program. J Immunol. 2015; 195: 1791-803.
40. Stone EL, Pepper M, Katayama CD, Kerdiles YM, Lai CY, Emslie E, et al. ICOS coreceptor signaling inactivates the transcription factor FOXO1 to promote Tfh cell differentiation. Immunity. 2015; 42: 239-51.
41. Staron MM, Gray SM, Marshall HD, Parish IA, Chen JH, Perry CJ, et al. The transcription factor FOXO1 sustains expression of the inhibitory receptor PD-1 and survival of antiviral $CD8^+$ T cells during chronic infection. Immunity. 2014; 41: 802-14.
42. Grogg KL, Attygale AD, Macon WR, Remstein ED, Kurtin PJ, Dogan S. Expression of CXCL13, a chemokine highly upregulated in germinal center T-helper cells, distinguishes angioimmunoblastic T-cell lymphoma from peripheral T-cell lymphoma, unspecified. Mod Pathol. 2006; 19: 1101-7.
43. Piccaluga PP, Agostinelli C, Califano A, Carbone A, Fantoni L, Ferrari S, et al. Gene expression analysis of angioimmunoblastic lymphoma indicates derivation from T follicular helper cells and vascular endothelial growth factor deregulation. Cancer Res. 2007; 67: 10703-10.

Cite this article as: Xu M, Wang F, Chen H, Liu L, Liu W, Yang Y, et al. Inactivation of FOXO1 induces T follicular cell polarization and involves angioimmunoblastic T cell lymphoma. Cancer Biol Med. 2019; 16: 743-55. doi: 10.20892/j.issn.2095-3941.2019.0115